ELSEVIER

Journal of Alloys and Compounds 446–447 (2007) 571–574

Journal of ALLOYS AND COMPOUNDS

www.elsevier.com/locate/jallcom

Phase stabilities of Pd-based alloys for membranes for hydrogen gas separation: A statistical thermodynamics approach

D.E. Nanu, A.J. Böttger*

Department of Materials Science and Technology, Delft University of Technology, Mekelweg 2, 2628 CD Delft, The Netherlands

Received 12 September 2006; accepted 9 November 2006
Available online 22 December 2006

Abstract

A statistical thermodynamics approach based on the cluster variation method (CVM) is put forward for designing new Pd-based membrane materials. The tetrahedron approximation of CVM coupled with effective pair potentials is used to describe the phase boundaries between α- and β-phases in Pd-alloys–hydrogen systems. The model takes into account the volume changes during α–β transitions, and the possible order–disorder transitions. In principle, the method allows to predict the phase boundaries of new, not yet synthesized, *ternary* alloys using effective pair potentials determined based on experimental data of known *binary* Pd-alloys.

Keywords: Interstitial alloys; Hydrogen absorbing materials; Phase diagrams; Thermodynamic modeling

1. Introduction

Commercial Pd-based membranes are not yet suitable for long-term use as repeated cycles of hydrogen absorption/desorption lead to embrittlement caused by the hydride formation and subsequent decomposition. The development of suitable Pd-based membranes requires new alloys that meet certain criteria such as, e.g. critical temperature for the hydride formation below operating conditions, high hydrogen solubility and permeability, minimal stress development, poisoning resistance, etc. The knowledge and prediction of the phase stability of the α-metal solid solutions and the β-hydride phases formed during hydrogen absorption in Pd-alloys is particularly important for this purpose. Although experimental data on hydrogen solubility and thermodynamic properties of hydrogen in numerous binary Pd-alloys are available in literature [1,2], data for hydrogen in ternary or multicomponent alloys, which are of interest for practical applications, are scarce or absent. In this paper a statistical thermodynamic approach for describing the phase stabilities in Pd-alloys–H systems is put forward.

Pd-alloys–hydrogen systems are interstitial solid solutions: Pd and many of its alloys (with small content of alloying elements) have fcc crystal structures. The hydrogen atoms occupy, in most of the cases, the octahedral interstitial sites formed by the close-packed metal lattice [3]. The occupation of interstitial sites may result in pronounced distortion of the metal matrix resulting in strain-induced interactions, which could lead to order–disorder transitions. Thus the thermodynamic modeling of such systems should be capable of describing these effects. The cluster variation method (CVM) [4–6], used in this work, provides a reliable way to estimate the configurational entropy and to predict thermodynamic properties of systems showing order–disorder transitions [6–10]. The tetrahedron approximation of CVM is applied to model the α–β phase boundaries and the site occupations in the β-hydride phase in Pd-alloys–H systems. In particular, the method is applied to the Pd–Ni–H and Pd–Rh–H systems. The calculated phase boundaries are compared with experimental data. The effect of alloying on hydrogen solubility and on the short range ordering (SRO) of H in the β-hydride phase is assessed. The method is further used to predict the α–β phase boundaries of ternary alloy–hydrogen systems (Pd–Ni–Rh–H) by using effective pair potentials of the binary alloys.

2. Methodology

The tetrahedron approximation of CVM is chosen to describe fcc Pd–M substitutional alloys containing interstitial hydrogen atoms. It is assumed that the

* Corresponding author. Tel.: +31 15 278 2243; fax: +31 15 278 6730.
E-mail address: A.J.Bottger@tudelft.nl (A.J. Böttger).

0925-8388/$ – see front matter © 2006 Published by Elsevier B.V.
doi:10.1016/j.jallcom.2006.11.071

Table 1
Effective Lennard–Jones parameters used to model the α–β phase boundaries in $Pd_{(100-x)}Ni_x$–H and $Pd_{(100-x)}Rh_x$–H systems

System	Pair	ε^0 (kJ/mol)	$\varepsilon^0/\varepsilon^0_{Vac-Vac}$	r^0 (nm)	$r^0/r^0_{Vac-Vac}$
	Vac–Vac	63.213	1.0000	0.27429	1.0000
$Pd_{95}Ni_5$–H	H–Vac		0.6810		1.0375
	H–H	22.416	0.3546	0.28902	1.0537
	Vac–Vac	63.623	1.0000	0.27328	1.0000
$Pd_{90.4}Ni_{9.6}$–H	H–Vac		0.6885		1.0390
	H–H	23.093	0.3630	0.29012	1.0616
	Vac–Vac	64.104	1.0000	0.27209	1.0000
$Pd_{85}Ni_{15}$–H	H–Vac		0.7000		1.0425
	H–H	23.891	0.3727	0.29345	1.0785
	Vac–Vac	64.238	1.0000	0.27478	1.0000
$Pd_{95}Rh_5$–H	H–Vac		0.6855		1.0370
	H–H	23.591	0.3673	0.29013	1.0558
	Vac–Vac	65.708	1.0000	0.27457	1.0000
$Pd_{90}Rh_{10}$–H	H–Vac		0.6930		1.0365
	H–H	25.246	0.3842	0.28907	1.0528

interstitial atoms only occupy the octahedral sites formed by the close-packed metal lattice. Hence the interstitial lattice has also an fcc structure. The system comprising two fcc sublattices (binary Pd–M metal lattice, and binary H–Vac interstitial lattice) is modeled as a binary H–Vac system in the effective field created by the metal lattice. The I-sublattice is subdivided into four interpenetrating fcc sublattices, denoted by α, β, γ and δ. For each of these four sublattices the site occupation is described by i, j, k and l, respectively. The indices i, j, k and l, can take the values of 1 or 2 whether the sites are occupied by H or Vac [11]. The distribution variables of the tetrahedron cluster are denoted by $Z_{ijkl}^{\alpha\beta\gamma\delta}$ and represent the probability that a tetrahedron has the configuration i, j, k, l, on the lattice sites α, β, γ, δ, respectively. The grand potential function, Ω, is used to calculate the equilibrium states. For each phase, the grand potential per lattice site is defined [7] as:

$$\Omega(V, T, \mu_1^*, \mu_2^*) = U - TS + pV - \sum_{n=1}^{2} \mu_n^* x_n + \lambda \left(1 - \sum_{ijkl} Z_{ijkl}\right) \quad (1)$$

where U and S describe the energy and the entropy per lattice site, respectively, T the temperature, p the external pressure, V the volume per lattice site, x_n the mole fraction of component n ($n = 1, 2$) in the phase considered and μ_n^* is the effective chemical potential defined as $\mu_n^* = \mu_n - (\mu_1 + \mu_2)/2$, where μ_n is the chemical potential of component n. The term $\lambda \left(1 - \sum_{ijkl} Z_{ijkl}\right)$ expresses the constraint that the cluster distribution variables are normalized, λ being a Lagrange multiplier. The internal energy U and the entropy S of the system are described as functions of cluster and subcluster distribution variables [11]. The vibrational contributions to energy and entropy are not considered in the calculations. The internal energy is taken as the weighted sum of the internal energy of all occurring tetrahedrons. The internal energy of each tetrahedron is described as the sum of the pairwise interactions within the tetrahedron. An 8-4 type Lennard–Jones (L–J) potential is used to describe the volume dependence of the effective pair interactions [7]. The L–J parameters describing the H–H and Vac–Vac effective pair interactions are determined based on the cohesive energies and lattice parameters of, respectively, the fully hydrogenated and the hydrogen free alloys as described in [12]. The parameters describing the H–Vac effective pair interactions are obtained by fitting to the phase boundaries, i.e. the parameters were optimized by trial and error so to achieve a good agreement between the calculated and the experimental compositions at the phase boundaries at one temperature. The values of the L–J parameters used to describe the systems discussed in this paper are given in Table 1.

For a given temperature, T, and fixed effective chemical potentials, μ_n^*, the equilibrium state of the system corresponds to those configurations that minimize the value of the grand potential $\Omega(V, T, \mu_1^*, \mu_2^*)$. The natural iteration method [5,13] is used to minimize $\Omega(V, T, \mu_1^*, \mu_2^*)$ with respect to the cluster distribution variables and volume. Atmospheric pressure is taken as the reference pressure p. The thermodynamic equilibrium between two phases, here the α-solid solution and β-hydride phases, is determined by the T and μ^* for which the Ω's are the same for both phases. In this way the concentrations and the lattice parameters of the phases in equilibrium are determined.

3. Results and discussion

The phase boundaries between α-metal solid solutions and β-metal hydrides were calculated for a number of binary Pd–M alloys with different content of alloying element M. Correlations between the effective L–J parameters and the content of alloying element were derived and subsequently used to predict the phase boundaries in multicomponent Pd–M1–M2–H alloys. Due to space limitation we will discuss just a few examples, more results and further applications will be described in [12].

The calculated and experimental data of α–β phase boundaries for $Pd_{(100-x)}Ni_x$–H and $Pd_{(100-x)}Rh_x$–H systems are shown in Fig. 1. The phase boundaries calculated by using the L–J parameters given in Table 1 are represented by lines, the experimental data by symbols. The experimental data shown in Fig. 1 are the compositions at the phase boundaries (i.e. atomic ratio H/(Pd + M) contents at α_{max} and β_{min}) determined at a given T by extrapolation [14] from the pressure-composition isotherms reported in [15,16]. The calculated (α + β)/β phase boundaries are in better agreement with the experimental data than the α/(α + β) phase boundaries. Part of the discrepancy can be assigned to the difficulties in the determination of the experimental α_{max} because of (i) the very low (below 0.05 atomic ratio H/metal) H-content and (ii) the non-ideality of the solvus formation causing errors in the extrapolation. Nevertheless, the model seems to underestimates the α_{max} compositions at a given T, and also the temperature dependence of the α_{max} compositions seems to be not correctly described. This can most probably be attributed to the fact that the model

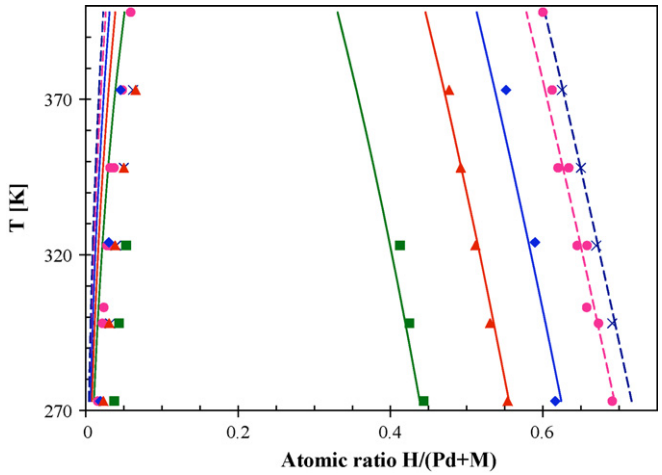

Fig. 1. Comparison of experimental (symbols) and calculated (lines) phase boundaries in $Pd_{(100-x)}Ni_x$–H with $x = 5$, 9.6 and 15 at.% Ni, and in $Pd_{(100-x)}Rh_x$–H systems with $x = 5$ and 10 at.% Rh. Symbols: experimental data for (♦) $Pd_{95}Ni_5$–H [15], (▲) $Pd_{90.4}Ni_{9.6}$–H [15], (■) $Pd_{85}Ni_{15}$–H [15], (●) $Pd_{95}Rh_5$–H [16], and (×) $Pd_{90}Rh_{10}$–H [16] systems. Lines: phase boundaries calculated with L–J parameters given in Table 1.

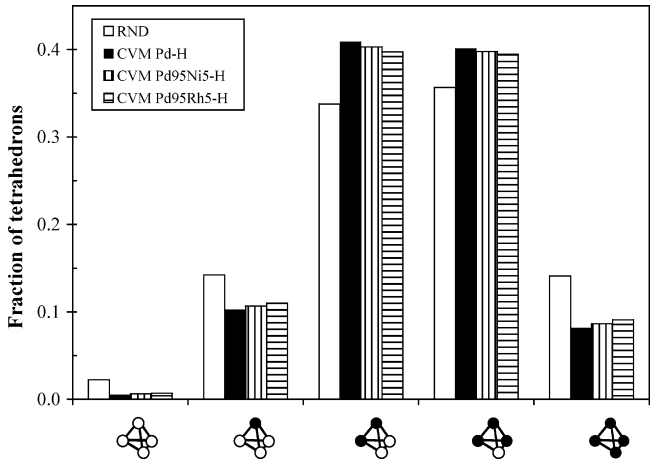

Fig. 2. Fraction of tetrahedron clusters containing 0–4 H atoms (●) or vacancies (◯) occurring in the β-hydride phase of $Pd_{(100-x)}M_x$–H systems for an H content of 38 at.% at 298 K as obtained from the CVM and for a random distribution.

does not take into account the elastic/vibrational effects. These generally bring phase boundaries of low interstitials containing alloys to higher compositions [17].

In view of the above, it can be concluded that the model describes well the *increase* of the maximum hydrogen solubility (α_{max}) in the α-phase, and the *decrease* of the minimum hydrogen absorption capacity (β_{min}) in the β-phase, with increasing Ni content in $Pd_{(100-x)}Ni_x$–H systems, as well the *increase* of the minimum hydrogen absorption capacity with increasing Rh content in $Pd_{(100-x)}Rh_x$–H systems.

The results shown in Fig. 1 demonstrate that the model is able to describe the effect of the choice of the alloying element (Ni and Rh) and its concentration on the phase boundaries. Similar results were obtained for the case of other Pd–M–H systems; some examples will be discussed in [12]. The analysis of the values of the L–J parameters used to calculate the phase boundaries in $Pd_{(100-x)}Ni_x$–H and $Pd_{(100-x)}Rh_x$–H systems shows that the strength of the effective field of the metal sublattice and the relative interaction strength between nearest-neighbor occupied (H) and unoccupied (Vac) interstitial sites determine the phase boundaries (see Table 1).

The relative interaction strength between hydrogen and vacancies could also induce SRO in the β phase. This is demonstrated by comparing the site occupancies of the tetrahedron clusters calculated for a fixed composition and T from the cluster distribution variables $Z_{ijkl}^{\alpha\beta\gamma\delta}$ obtained by CVM, with those corresponding to a random distribution of atoms at the same composition (here taken as 38 at.% H = 0.61 atomic ratio H/(Pd + M)). In Fig. 2 the presence of SRO at room temperature in the β phase of Pd and Pd–M alloys is obvious. In all cases, the CVM results indicate a larger fraction of tetrahedrons occupied with two or three H atoms, and a smaller fraction of empty tetrahedrons and tetrahedrons occupied by one or four H atoms than those of a random distribution. Moreover, a small effect of the alloying element on the occupation of tetrahedrons with respect to those in Pd can also be observed.

For the given $Pd_{(100-x)}M_x$–H systems, the L–J parameters used to describe the phase boundaries are found to depend linearly on the concentration of alloying element. Based on these relations the L–J parameters for any metal content can be estimated and used to predict the corresponding phase boundaries. Furthermore, the L–J parameters obtained for binary Pd-M alloys with hydrogen can be used to predict the L–J parameters for ternary or multicomponent Pd-alloys with hydrogen, thereby using the weighted averages of all the L–J parameters of the corresponding pairs of the binary Pd-alloys included in the multicomponent alloy.

Some examples of predicted (α + β)/β phase boundaries in $Pd_{(100-2x)}Ni_xRh_x$–H systems, with $x = 2.5$ and 5 at.% are shown in Fig. 3. In these cases the L–J parameters are obtained by averaging the L–J parameters used to describe the $Pd_{(100-x)}Ni_x$–H

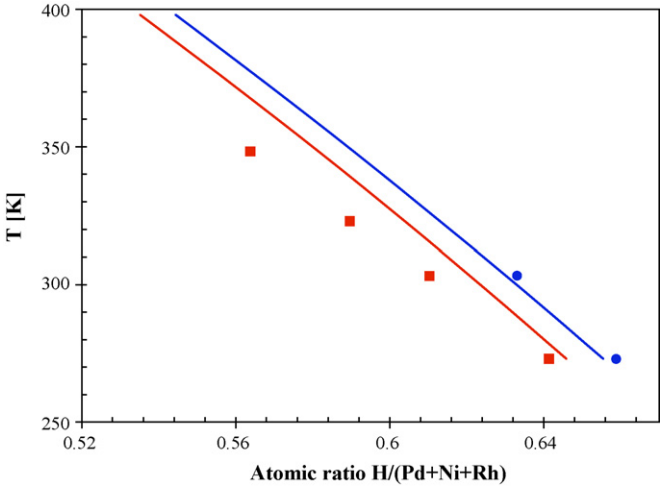

Fig. 3. Prediction of the (α + β)/β phase boundaries in $Pd_{(100-2x)}Ni_xRh_x$–H systems. Symbols: experimental data for (●) $Pd_{95}Ni_{2.5}Rh_{2.5}$–H [18], (■) $Pd_{90}Ni_5Rh_5$–H [18] systems. Lines: predicted phase boundaries (see text for explanations).

and $Pd_{(100-x)}M_x$–H systems. The calculated phase boundaries are in rather good agreement with the experimental results. These results suggest that the present approach allows to predict the α–β phase boundaries of new, not yet synthesized, ternary alloys.

4. Conclusions

The tetrahedron approximation of CVM coupled with effective pair potentials is successfully used to describe the α–β phase boundaries in Pd–M–H systems (M = Ni, Rh). The calculations show that the strength of the effective field of the metal sublattice and the relative interaction strength between nearest-neighbor occupied and unoccupied interstitial sites determine the phase boundaries and degree of short-range order. The method also allows to predict the α–β phase boundaries of ternary Pd–Ni–Rh–H alloys using effective pair potentials obtained from experimental data of the corresponding binary alloys. In principle the approach allows the prediction of phase boundaries of new multicomponent alloys provided that data on the binary alloys is available.

Acknowledgements

A grant from Senter Novem in the framework of the EDI (Energiebesparing Door Innovatie) program is gratefully acknowledged. This work is also part of a research program of the Netherlands Institute for Metals Research (NIMR) and the Stichting voor Fundamenteel Onderzoek der Materie, FOM, financially supported by the Nederlandse Organisatie voor Wetenschappelijk Onderzoek (NWO).

References

[1] Y. Sakamoto, F.L. Chen, M. Ura, T.B. Flanagan, Ber. Bunsen Ges. Phys. Chem. 99 (1995) 807–820.
[2] T.B. Flanagan, Y. Sakamoto, Platinum Met. Rev. 37 (1993) 26–37.
[3] I.E. Worsham, M.K. Wilkinson, C.G. Shull, J. Phys. Chem. Solids 3 (1957) 303–310.
[4] R. Kikuchi, Phys. Rev. B 81 (1951) 988–1003.
[5] R. Kikuchi, J. Chem. Phys. 60 (1974) 1071–1080.
[6] D. De Fontaine, in: H. Ehrenreich, D. Turnbull (Eds.), Solid State Physics, vol. 47, Academic Press, New York, 1994, pp. 33–176.
[7] J.M. Sanchez, J.R. Barefoot, R.N. Jarrett, J.K. Tien, Acta Metall. 32 (1984) 1519–1525.
[8] M. Enomoto, H. Harada, Metall. Trans. A 20 (1989) 649–664.
[9] T. Mohri, J.M. Sanchez, D. de Fontaine, Acta Metall. 33 (1985) 1171–1185.
[10] C. Colinet, in: J.L. Morán-López, J.M. Sanchez (Eds.), Theory and Applications of the Cluster Variation and Path Probability Methods, Plenum Press, New York, 1996, pp. 313–340.
[11] M.I. Pekelharing, A.J. Böttger, M.A.J. Somers, E.J. Mittemeijer, Metall. Mater. Trans. A 30 (1999) 1945–1953.
[12] D.E. Nanu, A.J. Böttger, Adv. Funct. Mater., submitted for publication.
[13] R. Kikuchi, D. de Fontaine, Proceedings of the Workshop on Application of Phase Diagrams in Metallurgy and Ceramics, NBS Gaithersburg, 1977, pp. 967–997.
[14] E. Wicke, H. Brodowsky, in: G. Alefeld, J. Volkl (Eds.), Hydrogen in Metals, Springer, Berlin, 1978, pp. 73–155.
[15] Y. Sakamoto, T. Matsuo, H. Sakai, T.B. Flanagan, Z. Phys. Chem. Neue Fol. 162 (1989) 83–96.
[16] A.K.M. Fazle Kibria, Y. Sakamoto, Int. J. Hydrogen Energy 25 (2000) 853–859;
Y. Sakamoto, Y. Haraguchi, M. Ura, F.L. Chen, Ber. Bunsen Ges. Phys. Chem. 98 (1994) 964–969.
[17] S. Shang, A.J. Böttger, Acta Mater. 53 (2005) 255–264.
[18] Y. Sakamoto, K. Ohira, N. Ishimaru, F.L. Chen, M. Kokubu, T.B. Flanagan, J. Alloy Compd. 217 (1995) 226–234.